Optically detected magnetic resonance of the red and near-infrared luminescence in Mg-doped GaN

M. W. Bayerl, M. S. Brandt,* O. Ambacher, and M. Stutzmann
Walter Schottky Institut, Technische Universität München, Am Coulombwall, D-85748 Garching, Germany

E. R. Glaser, R. L. Henry, A. E. Wickenden, and D. D. Koleske
Naval Research Laboratory, Washington D. C. 20375-5347

T. Suski, I. Grzegory, and S. Porowski
High Pressure Research Center, Polish Academy of Sciences, Sokolowska 29, 01-142 Warsaw, Poland
(Received 25 May 2000; revised manuscript received 17 October 2000; published 12 March 2001)

We report photoluminescence (PL) and optically detected magnetic resonance (ODMR) measurements on magnesium-doped GaN samples grown by metal-organic chemical vapor deposition, molecular beam epitaxy, and high-pressure–high-temperature synthesis. The samples exhibit at least three luminescence bands in the red-to-infrared spectral range with maxima at ≈1.75, ≈1.55, and below 1.4 eV. ODMR on these emission bands reveals two deep defects with isotropic g values of 2.001 and 2.006 and linewidths of 4–5 and 18–32 mT, respectively. Spectrally resolved ODMR experiments suggest that a donor-to-deep defect recombination is responsible for the transitions at 1.75 eV, while an acceptor-to-deep defect transition causes the PL bands with lower energy. The deep centers involved are attributed to defects with energy levels in the lower part of the band gap but close to the midgap region.

DOI: 10.1103/PhysRevB.63.125203 PACS number(s): 78.55.Cr, 61.72.Ji, 76.70.Hb

I. INTRODUCTION

Although the photoluminescence (PL) and magnetic resonance properties of GaN already have been extensively studied, the microscopic understanding of defects and dopants in this material is very limited. For example, the origin of the residual donor responsible for unintentional *n*-type doping of GaN is still uncertain, though it is commonly associated with residual oxygen and/or silicon donors. An issue particularly relevant for bipolar device applications of GaN is the limitation of the *p*-type doping efficiency when incorporating large amounts ($>5\times10^{19}\,\mathrm{cm}^{-3}$) of magnesium into the material.[1] In this context it would be important to determine whether compensating defects such as the nitrogen vacancy or incorporation of Mg on nonsubstitutional lattice sites, e.g., in complexes or on interstitial lattice sites, is responsible for this limitation. The presence of compensating centers in Mg-doped GaN has already been shown by capacitance spectroscopy.[2,3] Even more sensitive to such deep defects should be PL experiments, which in GaN are expected to give rise to luminescence bands in the red or infrared spectral region. Indeed, several emission bands below 2 eV have been observed in GaN, most of them caused by transition metal impurities[4–6] or by defects generated through electron irradiation.[7,8] Additionally, a broad PL band at ≈1.7 eV has been found to be related to Mg doping. This band vanishes upon annealing at ≈700 °C.[9,10] Recently Kaufmann *et al.* have suggested a recombination model for a similar PL band at ≈1.8 eV in Mg-doped GaN intentionally compensated with Si.[11] Microscopic information about the different defects involved in subbandgap recombination can be obtained with optically detected magnetic resonance (ODMR). Such experiments generally can be used as decisive tests for different recombination models via the magnetic fingerprint of electronic levels involved in the recombination mechanism.

In this work, we investigate the photoluminescence and ODMR properties of Mg-doped GaN prepared by different growth techniques, with particular focus on the energy range from 2.0 to 1.1 eV (red to near-infrared luminescence). A variety of PL bands below 2 eV are found. The ODMR of these bands reveals several paramagnetic centers involved in the underlying radiative transitions, such as the center referred to as MM1 reported in an earlier publication.[12] Based on the PL and ODMR experiments, we propose models for the red and near-infrared luminescence observed from Mg-doped GaN.

II. EXPERIMENTAL DETAILS

Photoluminescence and optically detected magnetic resonance experiments were performed on a series of Mg-doped wurtzite GaN samples prepared by three different methods: epitaxial layers grown by metal-organic chemical vapor deposition[13] (MOCVD) and molecular beam epitaxy[14] (MBE) on sapphire, and bulk material grown by a high-pressure–high temperature process (HPHT).[15] The two MOCVD layers investigated were doped with $(2-5)\times10^{19}\,\mathrm{cm}^{-3}$ Mg atoms and had GaN layer thicknesses of 1.2 μm (MOCVD-I) and 3 μm (MOCVD-II). These two samples were grown at deposition pressures of 250 and 49 Torr, respectively. Subsequent secondary-ion mass spectroscopy (SIMS) studies on similar samples revealed a variation of unintentional silicon incorporation from approximately $8\times10^{16}\,\mathrm{cm}^{-3}$ for layers grown at deposition pressures near 50 Torr to approximately $3\times10^{17}\,\mathrm{cm}^{-3}$ for layers grown under pressures near 250 Torr. A conventional postgrowth thermal anneal procedure was performed to activate the Mg acceptors. Afterwards, both samples exhibited *p*-type conductivity

TABLE I. Compilation of the Mg as well as the Si and O impurity concentrations of the investigated samples. The concentrations were determined by SIMS for the MOCVD and MBE samples and by elastic recoil detection analysis for the bulk crystals.

Sample designation	[Mg] (cm^{-3})	[Si] (cm^{-3})	[O] (cm^{-3})
MOCVD-I	$(5.0\pm0.5)\times10^{19}$	$\sim(3.0\pm0.5)\times10^{17}$	$(1.5\pm0.5)\times10^{17}$
MOCVD-II	$(2.0\pm0.5)\times10^{19}$	$\sim(8.0\pm0.5)\times10^{16}$	
MBE-I	$(1.7\pm0.5)\times10^{20}$	$<1\times10^{18}$	
MBE-II	$(3.4\pm1.0)\times10^{20}$	$<1\times10^{18}$	
Bulk I	$(5.0\pm1.0)\times10^{19}$	$(1.0\pm0.2)\times10^{19}$	$(1.2\pm0.8)\times10^{20}$
Bulk II	$(5.0\pm1.0)\times10^{19}$	$(1.0\pm0.2)\times10^{19}$	$(1.2\pm0.8)\times10^{20}$

at room temperature as confirmed by Hall effect or thermoelectric probe measurements.

The two MBE samples had Mg concentrations of $1.7\times10^{20}\,cm^{-3}$ (MBE-I) and $3.4\times10^{20}\,cm^{-3}$ (MBE-II) and a thickness of 0.8 μm. Thermopower[16] and room-temperature Hall effect experiments proved that the MBE-II layer was *p*-type conductive with a hole concentration of $1\times10^{18}\,cm^{-3}$, while the more lightly doped MBE-I sample revealed a hole concentration of only $5\times10^{16}\,cm^{-3}$. Again, Mg concentrations in the MBE samples were determined by secondary-ion mass spectroscopy.

For the two bulk samples (bulk I and bulk II, thickness >100 μm), elastic recoil detection analysis experiments showed a Mg concentration of the order of $5\times10^{19}\,cm^{-3}$, but also revealed silicon impurities at a few times $10^{19}\,cm^{-3}$ and oxygen impurities between 5×10^{19} and $2\times10^{20}\,cm^{-3}$. Due to these high residual donor concentrations, the bulk samples were either fully compensated or still *n* type. The Mg, Si, and O concentrations of the samples are summarized in Table I.

PL and ODMR experiments were carried out at 5 K using the 351-nm line (i.e., 3.53 eV) of an Ar^+-ion laser for excitation. This provides an optical penetration depth of ~1 μm. The PL spectra were obtained with a 0.8-m double-grating monochromator and a GaAs photomultiplier tube. All PL spectra were corrected for the spectral response of the spectrometer. Typical PL excitation power densities were between 1 mW/cm^2 and 1 W/cm^2. The ODMR experiments were performed in a 34-GHz *Q*-band electron spin resonance (ESR) spectrometer in Voigt geometry ($\mathbf{k}\perp\mathbf{B}$, where $\mathbf{k}$ corresponds to the light propagation vector and $\mathbf{B}$ to the dc magnetic field) at microwave powers of 200 mW. For sensitive detection of the ODMR, additional power stabilization of the laser was employed. The overall luminescence intensity was monitored with a thermoelectrically cooled Si avalanche photodiode using low-pass or band-pass filters. The ODMR signal was detected by a lock-in amplifier in phase with the on-off modulation of the microwave. The best signal-to-noise ratios were achieved at optical excitation power densities of 1 W/cm^2 and microwave modulation frequencies of 1 kHz. Relative changes of the luminescence of 10^{-4} could be detected in a single scan. A maximal ODMR signal intensity $\Delta I/I=4\times10^{-4}$ was found in sample MOCVD-I. Unless otherwise noted, samples were mounted with the GaN crystallographic *c* axis perpendicular to the applied dc magnetic field.

III. RESULTS

A. Photoluminescence

The low-temperature photoluminescence of the six samples is given in Fig. 1. The dominant emission observed from the MOCVD samples consists of two broad overlapping luminescence bands of varying strength peaked at $\sim$2.8 and 3.1 eV. Both bands have similar intensities for MOCVD-I, whereas the 2.8-eV band dominates the emission of MOCVD-II, (the 3.1-eV band only gives rise to a small shoulder in this sample). In MOCVD material, the 2.8-eV ''blue'' band is often present in heavily Mg-doped samples

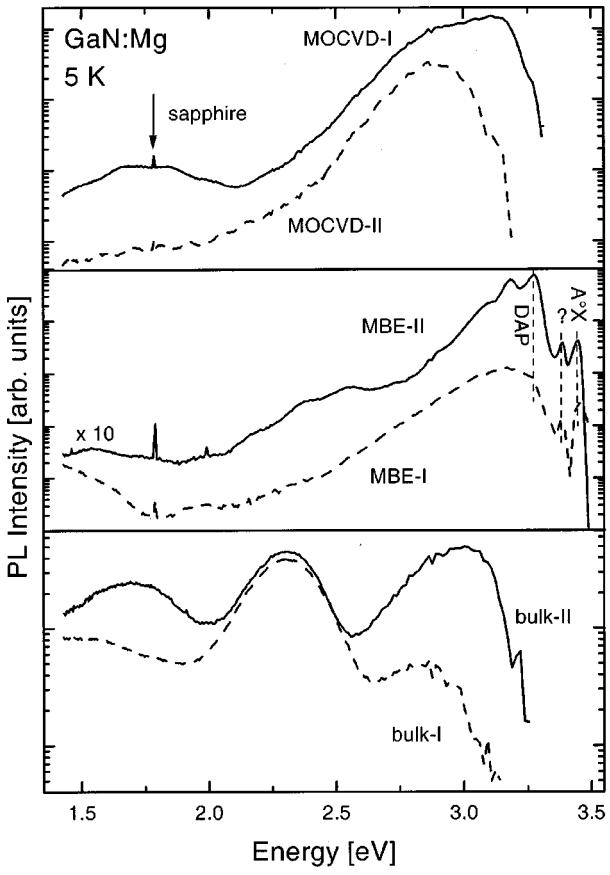

FIG. 1. Photoluminescence spectra at 5 K of the six Mg-doped GaN samples. In addition to the strong near-uv and blue luminescence bands, several emission bands in the ''red'' and ''near-infrared'' region are observed as well.

($[\mathrm{Mg}] > 2\times10^{19}\,\mathrm{cm}^{-3}$).[11] Based on the strong blueshift under high excitation powers[17] and thermal quenching behavior, this emission has been assigned to a deep-donor–shallow-acceptor recombination process with $E_d \approx 0.3-0.4\,\mathrm{eV}$.[18] The nature of the 3.1-eV band is still under discussion. One possibility is that, in contrast to the shallow-donor–shallow-acceptor (SD-SA) transition at 3.27 eV that is observed in lightly Mg-doped MOCVD material and *n*-type (compensated) material as well, a deeper donor level is involved in this recombination. Another, more recent model suggests that potential fluctuations due to a random distribution of charged acceptors and donors can cause a reduction of the peak energy and broadening of the 3.27-eV SD-SA band in the case of high Mg concentrations and high levels of compensating donors.[18]

In addition to the blue PL, the MOCVD-I sample exhibits a broad red luminescence band peaked around 1.75 eV. The Gaussian shape of this emission likely arises from strong electron-phonon coupling.[19] Such a PL band has been reported for GaN intentionally co-doped with Mg and Si, at donor and acceptor concentrations both well above $10^{18}\,\mathrm{cm}^{-3}$.[11] In contrast, sample MOCVD-II only shows weak luminescence in this spectral region. The periodic modulation at low PL energies in both samples is due to interference effects, whereas the sharp feature at 1.78 eV is caused by a chromium-related transition from the sapphire substrate.

The PL behavior of the MBE samples is distinctly different from the PL found for the MOCVD samples. In particular, two excitonic luminescence features are observed at 3.449 and 3.388 eV. The emission at 3.449 eV is similar to that reported for excitons bound to shallow Mg acceptors (A^0X) in GaN.[20] The origin of the line at 3.338 eV is unknown at this time but is likely associated with excitons bound to deeper impurities or complexes.

Below the excitonic regime, sample MBE-I exhibits a broad PL band at 3.1 eV. However, sample MBE-II shows a pronounced SD-SA recombination at 3.27 eV accompanied by 91-meV LO-phonon replicas typically found in lightly Mg-doped MOCVD layers.[11] If deep donors participate in the 2.8-eV luminescence band, this behavior would suggest that the formation of these donors is suppressed for the MBE growth, perhaps due to the different growth kinetics and the lower deposition temperatures. On the other hand, the model of Mg-induced potential fluctuations mentioned above would imply that the concentration of compensating donors in MBE-I is greater than in MBE-II.

Sample MBE-II shows an additional peak at approximately 2.5 eV. Indeed, a PL band with energy as low as 2.45 eV has been reported for Mg-doped GaN grown by hydride vapor phase epitaxy (HVPE) upon excitation with very low power densities of ($\approx 20\,\mathrm{mW/cm}^2$).[21] In contrast, the PL excitation power densities in this work are considerably larger and the strong power-dependent peak shift (>100 meV) reported for the 2.45-eV band has not been observed here. This suggests that the 2.5-eV feature in the MBE-grown material is not related to the 2.45-eV donor-acceptor pair (DAP) band reported in Ref. 21. In contrast, it may be associated, for example, with an internal transition of a single defect or complex.

Both MBE samples exhibit broad luminescence bands in the near-infrared region. While the PL maximum of sample MBE-II is located at ≈1.55 eV, the PL peak of the other layer is below the detection limit of 1.4 eV.

Finally, the bulk crystals show three broad luminescence bands of varying strength. The highest energy band peaks between 2.9 and 3.0 eV. Unlike the MOCVD and MBE samples, the bulk crystals show an additional strong ''yellow'' luminescence band with peak energy at 2.3 eV. In contrast to the 2.2-eV yellow luminescence in *n*-type GaN whose microscopic origin is still under discussion, the yellow band in Mg-doped GaN HPHT samples may be caused by the formation of Mg-O complexes[22,23] due to the high concentration of residual oxygen donors. The bulk crystals also exhibit luminescence below 2 eV with peaks at ~1.7 and ~1.5 eV for samples bulk II and bulk I, respectively.

B. ODMR

The ODMR of the strong blue or near-uv photoluminescence bands from these Mg-doped GaN samples exhibits previously reported donor and acceptor resonances.[5,12,24–26] The donors are typically characterized by g values between 1.949 and 1.962 depending on the sample, showing a small anisotropy ($\Delta g \equiv g_\parallel - g_\perp \sim 0.003-0.006$) and varying full widths at half maxima (FWHM) of ~5–17 mT. The comparatively larger anisotropy of the acceptor g values depends on various sample parameters such as the acceptor concentration,[25,27,28] the layer strain,[29] and the detection energy.[30] However, the main purpose of the present work is the investigation of the ODMR spectra measured on the red and near-infrared luminescence bands. Therefore, we will not pursue a detailed analysis of the results obtained for the blue PL.

The ''red'' ODMR spectra of the six samples with $B\perp c$ are shown in Fig. 2. For better comparison the ODMR signal intensities have been normalized. The respective optical detection range is indicated next to each spectrum. All ODMR resonances observed in this work are summarized in Table II.

Among the samples studied, the ODMR for MOCVD-I, MOCVD-II, MBE-I, and bulk I samples exhibit very similar line shapes, indicating that the processes observed are characteristic for the particular material studied rather than the deposition method used. The dominant features are luminescence-enhancing Gaussian-shaped lines with g values of 1.950, 1.959, 1.978, and 2.001. The first two signals have been attributed to shallow donors.[26,27] A similar $g = 1.978$ line was found previously in ODMR of the broad 3.0-eV emission band from high-resistivity GaN epitaxial layers and was assigned to quasishallow-donor states.[31] The $g = 2.001$ resonance, further called MM1, was tentatively assigned to a deep defect state in a previous publication,[12] in which the red luminescence was suggested to arise from a transition between a donor and the MM1 defect.

The MM1 resonance has a remarkably narrow FWHM of 4–5 mT, which is at least a factor of 3 smaller than the

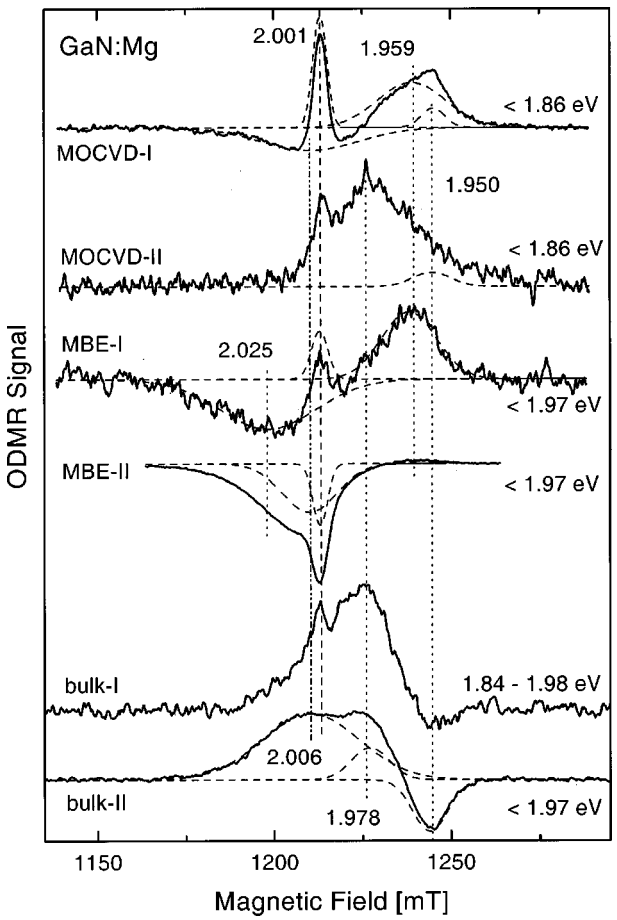

FIG. 2. ODMR of the GaN:Mg samples with $B \perp c$. Six different centers, indicated by dashed and dotted lines, influence the recombination processes responsible for the red and near-infrared emission bands. In particular, each spectrum includes either the MM1 (g=2.001) or MM2 ($g=2.006$) deep defect.

15–20 mT reported for other defect and acceptor resonances in GaN. As the linewidths were found to be independent of microwave frequencies,[24,32] an inhomogeneous broadening due to an unresolved hyperfine interaction was suggested to dominate the widths of those resonance lines. The MM1 signal thus seems to be much less affected by this broadening mechanism. The only other exception to such strong hyperfine broadening in GaN was found for the slightly anisotropic em-donor resonance detected on the 2.2-eV ''yellow'' PL band with a FWHM of ≈2–4 mT [first observed by conventional ESR experiments in *n*-type GaN with a FWHM of ≈0.5 mT (Ref. 33)].

There is a contribution to the high-field part of the spectra of samples MOCVD-I, MOCVD-II, bulk I, and bulk II from the em donor ($g_\perp = 1.950$), however with a considerably broader width of 8.5 mT, which probably results from lifetime broadening. This line has a luminescence-enhancing character for MOCVD-I and MOCVD-II, but a quenching effect on the PL from samples bulk I and bulk II. A reduction of the excitation power density for samples bulk I and bulk II decreases this quenching contribution until it vanishes, but a change from quenching to enhancing was not observed even for the lowest usable excitation powers. A model for the reversal in sign of this resonance will be discussed below.

In addition to the luminescence-enhancing lines at $g = 1.950$, 1.959, and 2.001 a weak quenching resonance with a g value of 2.006 (further called MM2) is resolved in sample MOCVD-I. These four lines can be separated using different optical excitation power densities: under higher excitation power, the relative intensity of the $g = 1.959$ enhancing and the quenching MM2 line increases. The MM2 resonance is isotropic within experimental accuracy and therefore distinguishable from the anisotropic shallow Mg acceptor resonance ($g_\perp \approx 2.016$; $g_\parallel \approx 2.056$) observed on the blue luminescence band of this sample. In sample bulk II the MM2 resonance is found as a luminescence-enhancing ODMR signal. This line is accompanied by an enhancing $g = 1.978$ donor signal, which was present in samples MOCVD-II and bulk I as well.

Another distinct quenching resonance is observed for sample MBE-I. Here, the luminescence-quenching process involves a different deep defect or a deep acceptor state with $g_\perp \approx 2.025$ and $g_\parallel \approx 2.036$.

In contrast to the other samples discussed so far, the ODMR below 2 eV of the MBE-II layer is dominated by PL-quenching signals. The MM1 and MM2 defect signals are both observed to resonantly reduce the PL intensity. The spectrum is asymmetrically broadened at the low-magnetic-

TABLE II. Compilation of the *g*-factors and the resonance line widths of donors, deep defects and acceptor-related ODMR signals observed in the samples studied in this work.

				ODMR below 2 eV in sample					
Defect	$g_\perp$	$g_\parallel$	$\Delta H_{1/2}$ (mT)	MOCVD-I	MOCVD-II	MBE-I	MBE-II	Bulk I	Bulk II
em donor	1.950	1.951	8–12	×	×			×	×
Shallow donor	1.959	1.962	18–23	×		×	×		
Quasishallow donor	1.978		14–22		×			×	×
MM1	2.001		4–5	×	×	×	×	×	
MM2	2.006		18–32	×			×	×	×
Acceptor	2.025	2.036	30			×	×		
Shallow Mg acceptor	2.00–2.02	2.04–2.08	20–30	Only observed for blue PL					

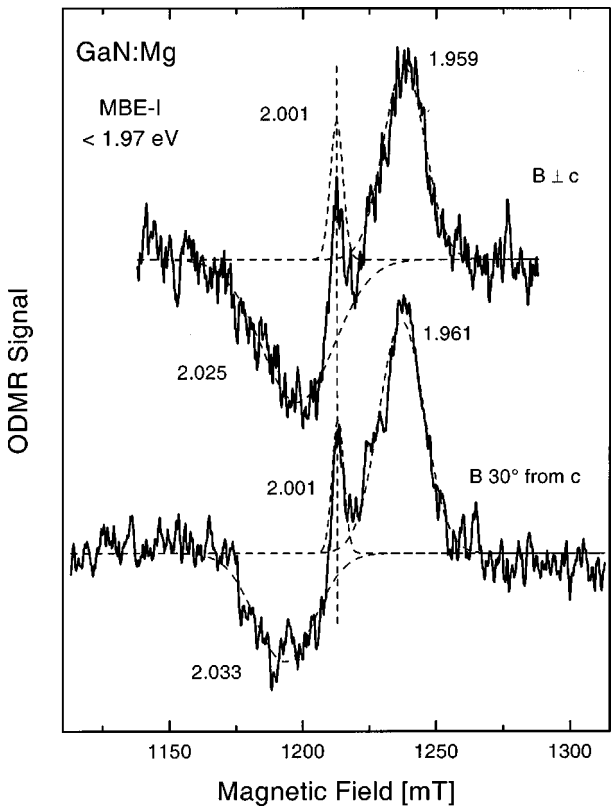

FIG. 3. Comparison of ODMR observed for sample MBE-I with $B \perp c$ and 30° from c. The MM1 resonance with $g = 2.001$ is found to be isotropic within the experimental accuracy of $\pm$ 0.001.

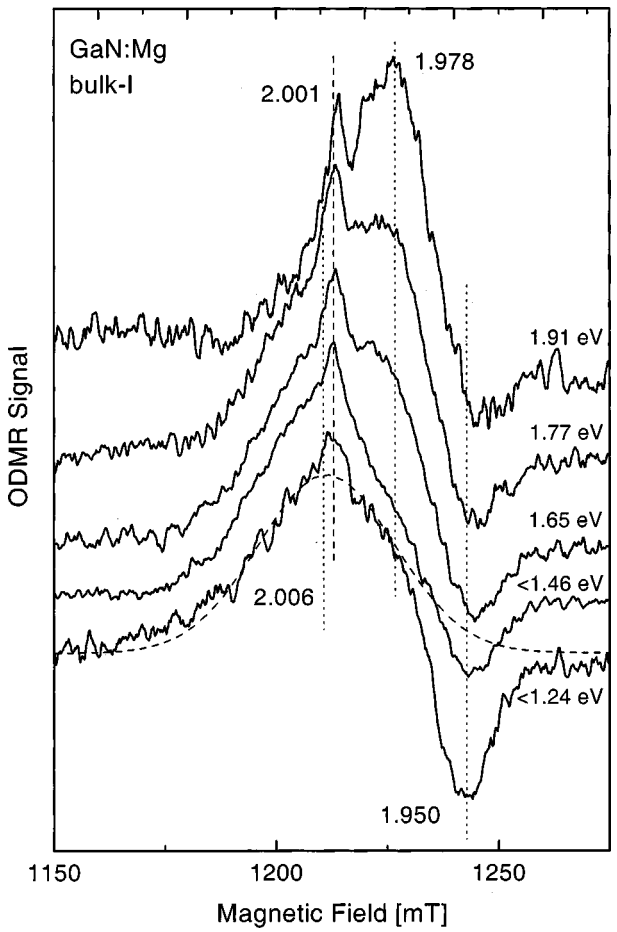

FIG. 4. Spectral dependence of the ODMR below 2 eV from sample bulk I with $B \perp c$. The ODMR on the emission near 2 eV is dominated by luminescence-enhancing resonances assigned to quasishallow donors ($g = 1.978$) and the MM1 deep defect ($g = 2.001$), whereas a lower energy process appears to involve the MM2 deep defect with $g = 2.006$.

field side, indicating that one or several acceptorlike resonances ($g > 2.01$) contribute to the PL-quenching process as well. There is only a very weak PL increasing component from the donor with $g_\perp \approx 1.959$.

The orientation dependence of the ODMR below 2 eV was identical for all six samples. As an example, spectra obtained for sample MBE-I with B oriented perpendicular and 30° from the c axis are shown in Fig. 3. In general, the shallow donors ($g = 1.95-1.96$) show a slight anisotropy as seen by the shift from $g_\perp = 1.959$ to $g_\parallel = 1.962$ in Fig. 3, whereas the ''quasishallow'' $g = 1.978$ donor, the MM1, and the MM2 deep defects are isotropic within the measurement accuracy of ± 0.001. The largest anisotropy is observed for the deep acceptorlike centers that give rise to quenching ODMR resonances for the MBE samples ($g_\perp \approx 2.025$ and $g_\parallel \approx 2.036$). However, this g anisotropy is still considerably smaller compared to that found for the shallow acceptors detected on the blue emission bands from these samples. The anisotropies of the g factors are also compiled in Table II.

Further information on the nature of the red and near-infrared luminescence is provided by spectrally resolved experiments. A series of ODMR spectra detected at different wavelengths for sample bulk I is shown in Fig. 4. We do not show the spectral dependence of the ODMR for the other samples, either because no significant variation of the ODMR with PL emission wavelength was observed (MOCVD-I, MBE-II) or because the red and infrared PL signals were too weak to allow observation of the ODMR spectral dependences (MOCVD-II, MBE-I). The spectra in Fig. 4 are vertically displaced and normalized to the same overall spin-dependent change for better comparability. While the upper three spectra were recorded using 1.91-, 1.77-, and 1.65-eV band-pass filters (approximate width of 0.2 eV), low-pass filters were used for the lower two spectra. The top spectrum is dominated by the $g = 1.978$ donor and the MM1 defect lines. Reducing the detection energy, the relative intensity of the $g = 1.978$ donor line decreases until, below 1.46 eV, it can no longer be resolved. As this line vanishes, the MM2 resonance, found as a quenching signal in the MOCVD-I and MBE-II samples, is observed as a strong enhancing line that seems to replace the $g = 1.978$ donor line. The relative intensity of the MM1 line, however, remains almost constant in all spectra. This indicates that at least two different PL processes are present. Both processes involve the MM1 defect, but the recombination step with higher PL energy includes the donors with $g = 1.978$, whereas the energetically lower transition includes the MM2 deep defect as the spin-dependent recombination partner. The detection wavelength dependence of the PL-quenching resonance with $g_\perp = 1.950$ will be discussed below.

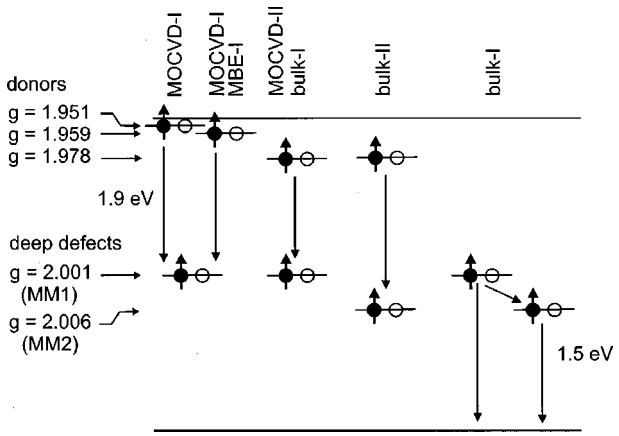

FIG. 5. Schematic diagram summarizing the recombination processes observed in the ODMR below 2 eV of various Mg-doped GaN samples.

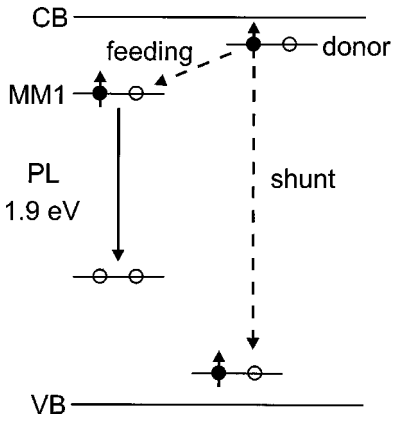

FIG. 6. Schematic diagram for a spin-dependent feeding process giving rise to an increase of the 1.9-eV photoluminescence (left-hand side) and a parallel shunt process that quenches the same emission (right-hand side). The full line represents the spin-independent PL recombination process involving a diamagnetic final state, while the dashed lines denote the spin-dependent transitions that are observed in the ODMR.

IV. DISCUSSION

A. Interpretation of the ODMR spectra: Energy levels and recombination processes

The recombination mechanisms revealed by ODMR of the red and infrared PL are quite complex. Various transitions from both acceptors and donors to deep traps are responsible for these bands. Furthermore, in some samples the different transitions are coupled through states that have more than one possible recombination partner influencing their respective transition rates and intensities. However, the recombination process causing the red and near-infrared luminescence appears very similar for samples MOCVD-I, MOCVD-II, MBE-I, and bulk I. The ODMR is dominated by luminescence-enhancing signals from a shallow donor and the MM1 defect. The particular donor involved is sample dependent and has g values of $g_\perp = 1.950$ (MOCVD-I, MOCVD-II), $g_\perp = 1.959$ (MOCVD-I, MBE-I), and $g = 1.978$ (MOCVD-II, bulk I). This suggests that the ODMR is caused by a spin-dependent transition between the respective donor and the MM1 deep defect. Therefore, the energy level of the paramagnetic state of the MM1 center is placed in the midgap region, about 1.9 eV below the conduction band.

In sample bulk II a similar recombination process governs the red PL. Here the spin-dependent recombination process includes the donor with $g = 1.978$ and the MM2 deep defect instead of the MM1 center. Therefore, MM2 (like MM1) is assigned to a defect with an energy level in the midgap region. Finally, the MM1 and the MM2 deep traps can also be involved in transitions with an acceptorlike state (not revealed in the ODMR), which gives rise to infrared emission (see, e.g., bottom spectrum in Fig. 4).

A summary of the PL-enhancing ODMR transitions described so far is given in Fig. 5. Here, the energy levels have been sorted according to their g values considering the g factor of shallow donors ($g_\perp = 1.950$) in GaN (Ref. 33) and assuming that deep states are typically characterized by g factors close to the free-electron value of 2.0023, since they do not reflect the symmetry of either the conduction or valence bands. The left-hand side of this picture concentrates on the higher-energy part of the sub-2-eV PL ($\approx$1.75 eV band). This PL band results from a transition between one of the three donors mentioned above and a deep defect (MM1 or MM2). One or more of these donors may be associated with the three different donor levels observed from Hall experiments (activation energies of 23.5, 52.5, and 110 meV) on unintentionally doped GaN.[34] The lower-energy, near-infrared part of the PL ($<$1.5 eV) is sketched on the right-hand side of this picture. Possible spin-dependent transitions leading to a luminescence enhancement include the MM1 to shallow-acceptor transition, and a MM1 or MM2 to valence-band transition. However, the valence-band resonance is not expected to be resolvable due to its short spin lifetime. Also a ''shallow'' acceptor resonance, as observed on the 3.27-eV SD-SA recombination in lightly Mg-doped MOCVD GaN,[27] might be too broad or too weak in terms of $\Delta I/I$ to be detectable. If both deep levels (MM1 and MM2) are present in one sample, the possible transfer of carriers from one deep level to the other and the relation with the actual luminescence band monitored has to be taken into account when analyzing the sign of the ODMR. An example for this will be given at the end of this section.

In samples MOCVD-I and MOCVD-II two donors simultaneously influence the PL. This implies that either a transition from each of the donors to the MM1 state is observed (as shown in Fig. 5) or that a spin-dependent feeding between the different donor levels enhances the red PL transition between the energetically deepest of the donor states and the MM1 deep defect. But at this point, also a spin-dependent feeding from a donor to the MM1 defect followed by a transition from the doubly occupied MM1 state to a deep level that generates the red PL cannot be ruled out (see left-hand side of Fig. 6). This alternative interpretation of the ODMR results is similar to the model proposed by Glaser *et al.* for the 2.2-eV ''yellow'' luminescence band.[24]

It is uncertain if the MM2 resonance observed in samples MOCVD-I, MBE-II, bulk II (see Fig. 2) and in sample bulk

I (see Fig. 4) is new or if it is of the same origin as the slightly anisotropic $L1$ level ($g_\perp = 2.004$, $g_\parallel = 2.008$) reported earlier for electron-irradiated GaN.[7,8] For the $L1$ center a shift of the peak position by 3 mT when changing the sample orientation from $B \| c$ to $B \perp c$ would be expected at Q band, which should be easily resolved. While the failure to observe an anisotropy for the MM2 resonance seems to exclude its assignment to $L1$, the influence of the high Mg doping level is unclear. The lattice distortion could lead to a significant reduction of the anisotropy, perhaps due to strain as suggested in the case of the shallow Mg-acceptor resonance.[25] The arithmetic average of $g_\perp$ and $g_\parallel$ for the $L1$ center is equal to the g value of 2.006 observed experimentally for the MM2 center. This and the similar linewidths of the resonances would, on the other hand, support an assignment of the MM2 line to the $L1$ resonance.

We will now discuss the PL quenching transitions. The fact that the ODMR of sample MBE-I is dominated by quenching lines in combination with the absence of a spectral dependence of the ODMR between 2.0 and 1.1 eV suggests that the transition energy of the parasitic process responsible for the quenching of the red PL is below the detection limit of 1.1 eV. A candidate for such a transition could be a deep level (e.g., the MM2 center) to deep-acceptor recombination monitored via the various red and near-infrared luminescence bands. In addition, spin-flip-induced nonradiative recombination is another possibility for such a shunt process.

The g values of the quenching line for sample MBE-I ($g_\parallel = 2.036$ and $g_\perp = 2.025$) are quite different from the isotropic g value of 2.006 observed for the MM2 center. Nevertheless, this anisotropy is still smaller than that found for the acceptorlike resonance detected on the blue band of the MBE-I sample ($g_\perp = 2.018$, $g_\parallel = 2.065$). Therefore the shallow Mg acceptor states involved in the blue PL transition are not responsible for the quenching lines observed on the red ODMR. The properties of deep acceptors, perhaps Mg-related as well, will not reflect the symmetry of the uppermost valence band alone. Thus, the g anisotropy is expected to be reduced compared to that associated with the shallow Mg acceptors.

We now offer some remarks concerning the reversal in sign of ODMR resonances. In general, quenching lines indicate the presence of competing pathways for charge carrier recombination. The relative intensities of the quenching and enhancing contributions are governed by the transition rates between all centers involved (more sophisticated models of ODMR are given elsewhere[35]). We explain this in more detail for the example of the $g_\perp = 1.950$ donor line. For this purpose let us recall the ODMR measurements of the MOCVD samples. The spectra are characterized by a transition from the $g_\perp = 1.950$ and a second donor to the MM1 defect. Therefore, all these lines are detected as luminescence-enhancing resonances. Now consider a second, parasitic recombination path involving the $g_\perp = 1.950$ donor. Such a shunt path would be, e.g., the recombination with a hole located in the valence band or at a shallow Mg acceptor state (see right-hand side of Fig. 6). The net effect of the PL-enhancing and -quenching contributions for the $g_\perp = 1.950$ resonance is determined by the relative transition rates of the respective recombination processes. In the case of the bulk samples the shunt process is faster than the red luminescence. Hence, the $g_\perp = 1.950$ donor line is observed as a PL-quenching signal.

For an evaluation of the expected sign and intensity of a resonance associated with a defect that takes part in both luminescence-enhancing and -quenching transitions, the coupled rate equations for all centers involved have to be solved. These depend on the stationary condition of the system at a given generation rate. This applies to the $g_\perp = 1.950$ donor in the bulk samples as well, as indicated by the pronounced excitation power dependence of the ODMR line shape. Due to the large number of donors and acceptors in these samples, higher excitation densities in this case lead to an increase of the number of electrons located at the $g_\perp = 1.950$ donor and holes located in the valence band or at shallow acceptor sites. Thus, the red PL is quenched via the $g_\perp = 1.950$ donor as soon as the lifetime of this donor is dominated by the recombination with holes in the valence band or at shallow acceptors rather than by the transition to the MM1 defect. The quenching effect becomes stronger when the excitation power is further increased.

B. The origin of the red and near-infrared luminescence

The recombination model of Kaufmann *et al.*[11] proposed for the red luminescence in Mg-doped GaN compensated with Si suggested that the 2.2-eV yellow and the 1.75-eV red luminescence bands both involve the *same* deep center as the final state of the electronic transition. According to their model, the initial states for both luminescence pathways are donors with a considerable difference in binding energies which accounts for the difference in PL energies. The present results cannot support this model. In particular, the ODMR experiments on the emission below 2 eV from these samples never revealed the typical deep defect with $g = 1.989$ commonly observed on the yellow luminescence band from *n*-type GaN.

The model that we propose is more complex due to the variety of PL bands and ODMR signals (see Table II) observed in this work. It is based on two deep defect levels, the MM1 center with $g = 2.001$ and a FWHM of 4–5 mT and the MM2 deep defect with $g = 2.006$ and a FWHM of 18–32 mT. ODMR measurements indicate that at least three different donor-to-MM1 transitions contribute to a broad emission band ranging from 1.5–2.0 eV. Furthermore, the 1.75-eV PL band is stronger in the MOCVD-grown samples with higher residual Si impurity levels, in agreement with the original observation by Kaufmann *et al.*[11] However, it cannot be decided whether the MM1 center is silicon-related or if just the higher concentration of Si donors induces the increased donor-to-MM1 recombination rate.

According to the ODMR results, the emission bands below 1.5 eV are assigned to transitions between the other deep defect (MM2) with $g = 2.006$ and the valence-band or ''shallow'' acceptors. These bands were only observed in the PL and ODMR experiments reported above from the MBE and bulk samples. The origin of this emission does not necessar-

ily have to be related to silicon, but also could arise from other impurities, such as oxygen or carbon. Indeed, the MBE layer with the higher carbon impurity concentration (MBE-I) exhibits stronger PL in this spectral range.

Dislocations, which in principle could give rise to sub-band-gap luminescence as well, can be ruled out as the origin of the reported PL bands below 2 eV, since this emission is also present in bulk material with low dislocation densities. But although the model involving spin-dependent recombination from a shallow donor to a deep defect and from a deep defect to a shallow acceptor for the 1.75-eV and below 1.5-eV PL bands, respectively, seems to be most consistent with the ODMR data, spin-dependent feeding processes such as that suggested for the yellow luminescence band in *n*-type GaN cannot be excluded.

V. CONCLUSIONS

PL and ODMR experiments have been performed on six Mg-doped GaN samples grown by MOCVD, MBE, and HPHT synthesis. The presence of deep levels causing red and near-infrared photoluminescence is demonstrated. These PL bands are broad and structureless with peak energies at $\approx$1.75, $\approx$1.55, and below 1.4 eV. The ODMR on these bands commonly shows the presence of two distinct deep levels. The first level, called MM1 with an isotropic g factor of 2.001, exhibits a remarkably narrow linewidth of 4–5 mT and is exclusively detected on the red luminescence bands. The second deep level involved in the red PL, called MM2, has an isotropic g value of 2.006 and a linewidth of 18–32 mT. It is similar to the $L1$ center found in e^--irradiated GaN but does not show the anisotropy reported for $L1$. Based on spectrally resolved experiments the MM1 and MM2 centers are attributed to deep defects with energy levels in the lower part of the midgap region.

ACKNOWLEDGMENTS

We thank W. Burkhardt and D. M. Hofmann (Universität Gießen) for the SIMS analyses of the MBE samples. We also thank J. A. Freitas, Jr. (NRL) for the initial low-temperature PL measurements and W. J. Moore (NRL) for transport measurements of the MOCVD samples. The work at the WSI was supported by the Deutsche Forschungsgemeinschaft through SFB 348.

*Email: martin.brandt@physik.tu-muenchen.de

[1] P. Kozodoy, H. Xing, S. P. DenBaars, U. K. Mishra, A. Saxler, R. Perrin, S. Elhamri, and W. C. Mitchel, J. Appl. Phys. **87**, 1832 (2000).

[2] W. Götz, N. M. Johnson, and D. P. Bour, Appl. Phys. Lett. **68**, 3470 (1996).

[3] G.-C. Yi and B. W. Wessels, Appl. Phys. Lett. **68**, 3769 (1996).

[4] K. Maier, M. Kunzer, U. Kaufmann, J. Schneider, B. Monemar, I. Akasaki, and H. Amano, Mater. Sci. Forum **143–147**, 93 (1994).

[5] M. Kunzer, U. Kaufmann, K. Maier, J. Schneider, N. Herres, I. Akasaki, and H. Amano, Mater. Sci. Forum **143–147**, 87 (1994).

[6] J. Baur, U. Kaufmann, M. Kunzer, J. Schneider, H. Amano, I. Akasaki, T. Detchprohm, and K. Hiramatsu, Appl. Phys. Lett. **67**, 1140 (1995).

[7] M. Linde, S. J. Uftring, G. D. Watkins, V. Härle, and F. Scholz, Phys. Rev. B **55**, R10 177 (1997).

[8] C. Bozdog, H. Przybylinska, G. D. Watkins, V. Härle, M. Kamp, R. J. Molnar, A. E. Wickenden, D. D. Koleske, and R. L. Henry, Phys. Rev. B **59**, 12 479 (1999).

[9] S. Nakamura, M. Senoh, and T. Mukai, Jpn. J. Appl. Phys., Part 2 **30**, L1708 (1991).

[10] S. Nakamura, N. Iwasa, M. Senoh, and T. Mukai, Jpn. J. Appl. Phys., Part 1 **31**, 1258 (1992).

[11] U. Kaufmann, M. Kunzer, H. Obloh, M. Maier, Ch. Manz, A. Ramakrishnan, and B. Santic, Phys. Rev. B **59**, 5561 (1999).

[12] M. W. Bayerl, M. S. Brandt, E. R. Glaser, A. E. Wickenden, D. D. Koleske, R. L. Henry, and M. Stutzmann, Phys. Status Solidi B **216**, 547 (1999).

[13] A. E. Wickenden, D. K. Gaskill, D. D. Koleske, K. Doverspike, D. S. Simons, and P. H. Chi, in Gallium Nitride and Related Materials, MRS Symposia Proceedings No. 395 (Materials Research Society, Pittsburgh, 1996), p. 679.

[14] H. Angerer, O. Ambacher, R. Dimitrov, Th. Metzger, W. Rieger, and M. Stutzmann, MRS Internet J. Nitride Semicond. Res. **1**, 15 (1996).

[15] S. Porowski and I. Grzegory, in GaN and Related Materials, edited by S. J. Pearton (Gordon and Breach, Amsterdam, 1997), Vol. 2, p. 295.

[16] M. S. Brandt, P. Herbst, H. Angerer, O. Ambacher, and M. Stutzmann, Phys. Rev. B **58**, 7786 (1998).

[17] U. Kaufmann, M. Kunzer, M. Maier, H. Obloh, A. Ramakrishnan, B. Santic, and P. Schlotter, Appl. Phys. Lett. **72**, 1326 (1998).

[18] M. A. Reshchikov, G.-C. Yi, and B. W. Wessels, Phys. Rev. B **59**, 13 176 (1999).

[19] D. B. Fitchen, in *Physics of Color Centers*, edited by W. B. Fowler (Academic, New York, 1968).

[20] S. Strauf, P. Michler, J. Gutowski, U. Birkle, M. Fehrer, S. Einfeldt, and D. Hommel, Phys. Status Solidi B **216**, 557 (1999).

[21] L. Eckey, U. von Gfug, J. Holst, A. Hoffmann, A. Kaschner, H. Siegle, C. Thomsen, B. Schineller, K. Heime, M. Heuken, O. Schön, and R. Beccard, J. Appl. Phys. **84**, 5828 (1998).

[22] M. W. Bayerl, M. S. Brandt, T. Suski, I. Grzegory, S. Porowski, and M. Stutzmann, Physica B **273–274**, 120 (1999).

[23] M. Godlewski, T. Suski, I. Grzegory, S. Porowski, J. P. Bergman, W. M. Chen, and B. Monemar, Physica B **273–274**, 39 (1999).

[24] E. R. Glaser, T. A. Kennedy, K. Doverspike, L. B. Rowland, D. K. Gaskill, J. A. Freitas, Jr., M. Asif Khan, D. T. Olson, J. N. Kuznia, and D. K. Wickenden, Phys. Rev. B **51**, 13 326 (1995).

[25] D. M. Hofmann, W. Burkhardt, F. Leiter, W. von Förster, H. Alves, A. Hofstaetter, B. K. Meyer, N. Romanov, H. Amano, and I. Akasaki, Phys. Rev. B **273–274**, 43 (1999).

[26] F. K. Koschnick, K. Michael, J.-M. Spaeth, B. Beaumont, P. Gibart, J. Off, A. Sohmer, and F. Scholz, J. Cryst. Growth **189/190**, 561 (1998).

[27] E. R. Glaser, T. A. Kennedy, J. A. Freitas, Jr., B. V. Shanabrook, A. E. Wickenden, D. D. Koleske, R. L. Henry, and H. Obloh, Physica B **273–274**, 58 (1999).
[28] M. Kunzer, J. Baur, U. Kaufmann, J. Schneider, H. Amano, and I. Akasaki, Solid-State Electron. **41**, 189 (1997).
[29] A. V. Malyshev, I. A. Merkulov, and A. V. Rodina, Fiz. Tverd. Tela (St. Petersburg) **40**, 1022 (1998) [Phys. Solid State **40**, 917 (1998)].
[30] E. R. Glaser (unpublished).
[31] E. R. Glaser, T. A. Kennedy, A. E. Wickenden, D. D. Koleske, and J. A. Freitas, Jr. in *III–V Nitrides*, MRS Symposia Proceedings No. 449 (Materials Research Society, Pittsburgh, 1997), p. 543.
[32] M. W. Bayerl, M. S. Brandt, and M. Stutzmann, Phys. Status Solidi A **159**, R5 (1997).
[33] W. E. Carlos, J. A. Freitas, Jr., M. Asif Khan, D. T. Olson, and J. N. Kuznia, Phys. Rev. B **48**, 17 878 (1993).
[34] V. A. Joshkin, C. A. Parker, S. M. Bedair, J. F. Muth, I. K. Shmagin, R. M. Kolbas, E. L. Piner, and R. J. Molnar, J. Appl. Phys. **86**, 281 (1999).
[35] B. C. Cavenett, Adv. Phys. **30**, 475 (1981).